Stem Cell Research (2014) 13, 300–315

Available online at www.sciencedirect.com

ScienceDirect

www.elsevier.com/locate/scr

REGULAR ARTICLE

Nanog induces hyperplasia without initiating tumors

Gerrit Fischedick[a,b], Guangming Wu[a], Kenjiro Adachi[a], Marcos J. Araúzo-Bravo[a,f], Boris Greber[a], Martina Radstaak[a], Gabriele Köhler[d], Natalia Tapia[a], Roberto Iacone[c,e], Konstantinos Anastassiadis[c], Hans R. Schöler[a,b,*], Holm Zaehres[a]

[a] *Department of Cell and Developmental Biology, Max Planck Institute for Molecular Biomedicine, Röntgenstrasse 20, 48149 Münster, Germany*
[b] *University of Münster, Faculty of Medicine, Domagstrasse 3, 48149 Münster, Germany*
[c] *Center for Regenerative Therapies, Technische Universität Dresden, Tatzberg 47-51, 01307 Dresden, Germany*
[d] *University of Münster, Gerhard-Domagk-Institut for Pathology, Domagkstraße 17, 48149 Münster, Germany*
[e] *F. Hoffmann-La Roche, Pharma Research and Early Development Discovery Technologies, 4070 Basel, Switzerland*
[f] *Biodonostia Health Research Institute, 20014 San Sebastián, and IKERBASQUE, Basque Foundation for Science, 48011 Bilbao, Spain*

Received 25 July 2014; accepted 4 August 2014
Available online date 10 August 2014

Abstract Though expression of the homeobox transcription factor Nanog is generally restricted to pluripotent cells and early germ cells, many contradictory reports about Nanog's involvement in tumorigenesis exist. To address this, a modified Tet-On system was utilized to generate Nanog-inducible mice. Following prolonged Nanog expression, phenotypic alterations were found to be restricted to the intestinal tract, leaving other major organs unaffected. Intestinal and colonic epithelium hyperplasia was observed—intestinal villi had doubled in length and hyperplastic epithelium outgrowths were seen after 7 days. Increased proliferation of crypt cells and downregulation of the tumor suppressors Cdx2 and Klf4 was detected. ChIP analysis showed physical interaction of Nanog with the Cdx2 and Klf4 promoters, indicating a regulatory conservation from embryonic development. Despite downregulation of tumor suppressors and increased proliferation, ectopic Nanog expression did not lead to tumor formation. We conclude that unlike other pluripotency-related transcription factors, Nanog cannot be considered an oncogene.

Introduction

Oct4, Sox2, and Nanog constitute the core transcriptional network of pluripotency. Acting together, these genes regulate self-renewal as well as the early stages of cellular differentiation both in vivo and in vitro (Boyer et al., 2005; Wang et al., 2006; Masui et al., 2007). Nanog expression is restricted to the developing embryo, where it is detectable in

* Corresponding author at: Max Planck Institute for Molecular Biomedicine, Röntgenstrasse 20, 48149 Münster, NRW, Germany. Fax: +49 251 70365 399.
E-mail address: office@mpi-muenster.mpg.de (H.R. Schöler).

http://dx.doi.org/10.1016/j.scr.2014.08.001
1873-5061/

the blastocyst until the formation of the epiblast and later on in the genital ridge during the formation of germ cells (Chambers et al., 2003; Mitsui et al., 2003). After birth, Nanog is undetectable in healthy somatic tissues but has been reported to be re-expressed in a number of somatic and germline tumors. There is mounting evidence suggesting that tumors are driven to grow by a small subfraction of cancer-inducing stem cells with the ability to initiate and maintain tumor growth and plasticity (Al-Hajj et al., 2003; O'Brien et al., 2007; Zhang et al., 2008; Hubbard and Gargett, 2010). Those studies led to investigations into tumor initiation and stemness, and subsequently to the hypothesis that certain tumors may arise from undifferentiated stem cells or that these undifferentiated stem cells undergo spontaneous de-differentiation to give rise to cancer-inducing cells (Reya et al., 2001; Beachy et al., 2004; Lobo et al., 2007; Stingl and Caldas, 2007). Gene expression analysis has recently been utilized to identify the re-activation of pluripotency-related markers in different human tumors. These studies have shown that similar global gene expression patterns in tumors and ES cells correlates with poorly differentiated and more aggressive tumors (Ben-Porath et al., 2008; Wong et al., 2008). Expression of pluripotency-related transcription factors such as Oct4 and Nanog has been associated with tumorigenesis in many reports, but the exact functional involvement of these factors in tumor progression and/or development has been controversial. For Oct4, many contradictory studies have been published depicting its presence or absence in different types of tumors (Tai et al., 2005; Atlasi et al., 2007; Ben-Porath et al., 2008; Cantz et al., 2008). However, in 2005 a study by Konrad Hochedlinger and colleagues finally clarified that Oct4 indeed has tumorigenic potential and can be considered to be an oncogene. In that study, the authors showed that ectopic expression of Oct4 in adult mice led to the formation of dysplastic lesions in the gut and invasive tumor growth in the skin (Hochedlinger et al., 2005). As for Oct4, Nanog expression has also been observed in different types of tumors, and its expression has been associated with aggressive tumor progression and poor patient diagnosis. Nanog-expressing tumors have been found in a wide variety of tissues, such as breast (Ezeh et al., 2005; Alldridge et al., 2008), cervix (Ye et al., 2008), kidney (Bussolati et al., 2008), oral cavity (Chiou et al., 2008), lung (Chiou et al., 2010), ovary (Zhang et al., 2008), gastric epithelium (Lin et al., 2012), pancreas (Wen et al., 2010), colon (Meng et al., 2010), and in germ cells (Gillis et al., 2011). A report by Jeter et al. analyzed the knockdown of Nanog in different cancer cell lines and found reduced clonal and clonogenic growth, reduced proliferation, and altered differentiation potential after Nanog ablation (Jeter et al., 2009). Although these publications alluded to a functional involvement of Nanog in tumor biology, many papers have reported that Nanog is confined to the cytoplasm, with no clear evidence of tumor-inducing functionality. Furthermore, systematic screens of different pluripotency-related transcription factors within patient tumor samples have shown that Nanog expression is not clinically relevant in colorectal cancer (Saiki et al., 2009). As a result, it remains unclear whether Nanog has oncogenic properties, in contrast to other transcription factors including Oct4. In light of these findings, we sought to clarify the role of Nanog in tumor formation and to this end generated a Nanog-inducible mouse line to investigate the tumor initiation potential of Nanog in the adult organism.

Material and methods

Plasmid construction

The murine Nanog cDNA was amplified by reverse transcription-polymerase chain reaction (RT-PCR) from ES cell cDNA using the primers Nanog_cDNA as shown in Table S1. The Nanog cDNA was cloned into a pCR2.1-TOPO plasmid (Invitrogen) and then cloned into a promoter-less pSport1 plasmid containing an SV40 polyadenylation sequence. This promoter-less plasmid was used to insert the tet-cmv_2-Insulator_PGK-Hygromycin cassette upstream of Nanog using Red/ET recombineering (Zhang et al., 1998, 2000).

Cell culture and production of tet-Nanog ES cells

Mouse ES cells were cultured in DMEM-KnockOut (Gibco, 10829018), containing 15% fetal calf serum (FCS; Biowest, Cat. S1810-500, Lot. S04595S1810), 1× penicillin/streptomycin/glutamine (PAA, P11-013), 1× nonessential amino acids (PAA, M11-003), and 50 μM 2-mercaptoethanol (Gibco, 31350010) on 0.1% gelatin-coated (Sigma, G1393) plates. Unless otherwise indicated, medium was supplemented with 1000 units/ml of leukemia inhibitory factor (LIF; home-made). For the production of the tet-Nanog ES cells, ES cells carrying the Oct4-GFP transgene from OG2 mice were used (Yoshimizu et al., 1999; Szabó et al., 2002). The transactivator CAGGs-irtTA-GBD*-IRES-puro (Anastassiadis et al., 2010) and the tet-responsive Nanog transgenes were sequentially electroporated into the cells using the Nucleofection II device from Amaxa. Electroporation was performed according to the manufacturer's instructions, and subsequent selection was performed with puromycin (1 μg/ml; Sigma P8833) and hygromycin (200 μg/ml; Roth Cp12.2). Clonal cell lines were established and tested for transgene induction.

Generation of tet-Nanog mice

ES cells were aggregated and cultured with denuded 8-cell-stage mouse embryos as described by Nagy and Rossant (Nagy et al., 2002) with slight modifications. Briefly, 8-cell embryos were flushed from (C57BL/6 × C3H) F1 female × CD1 male mice at 2.5 days post coitum (dpc) and placed in M2 medium (Nagy et al., 2002). Clumps of 8–15 loosely connected ES cells from short trypsin-treated day-2 ES cell cultures were chosen and transferred into small drops of potassium simplex optimized medium (KSOM medium) (Summers et al., 2000) with 10% FCS under mineral oil; each clump was placed in a depression in the drop. Meanwhile, batches of 30–50 embryos were briefly incubated in acidified Tyrode's solution (Nagy et al., 2002) until dissolution of their zona pellucida. A single embryo was placed on each clump of ES cells. All aggregates were assembled in this manner and cultured overnight at 37 °C, 5% CO_2 to allow the ES cells to integrate into the embryos. Finally, 11–14 aggregates were transferred into the uterine horns of each 2.5-dpc pseudopregnant foster mother (CD1 female × vasectomized CD1 male mice). The chimeric pups were delivered by natural birth or Cesarean section at 19.5 dpc and set up with foster mothers. Cells in culture were induced with 1 μg/ml of doxycycline (Sigma, D9891) and

1×10^{-7} M dexamethasone (Sigma, D1756). Mice were induced by intraperitoneal injection of 2 mg doxycycline (Sigma, D9891) and 0.5 mg dexamethasone (Sigma, D1756) or 0.63 mg dexamethasone-21-isonicotinate (Boehringer Ingelheim) every other day.

Protein and RNA preparation from organ samples

Samples of mouse organs were immediately frozen in liquid nitrogen after dissection. The organ samples were stored at −80 °C before being homogenized using the Precellys 24-Dual Homogenizer from Peqlab. Homogenization of the RNA samples was done in RLT Buffer (QIAGEN) followed by RNA extraction using the QIAGEN RNeasy Mini Kit. Protein samples were homogenized in RIPA Buffer (Sigma, R0278) in the presence of proteinase inhibitors (Roche, 11836153001). Protein content was measured using the Pierce 660 nm Protein Assay (Thermo Scientific, 22660).

Western blot analysis

Protein samples were boiled in SDS sample buffer and separated by a 12.5% SDS-PAGE and blotted onto polyvinylidene fluoride (PVDF) membranes. 25 μg of total protein extract was used per lane. Primary antibodies were anti-Nanog (1:500 dilution; Abcam, ab80892) and anti-Gapdh (1:10,000 dilution; Ambion, 4300). Secondary antibodies were anti-rabbit HRP (1:20,000 dilution; GE Healthcare, NA934) and anti-mouse HRP (1:20,000 dilution; Dianova, 115-035-044).

Histologic and immunohistochemical analyses

Tissue samples were fixed in 4% paraformaldehyde for 48–72 h at 20 °C. Samples were then dehydrated and embedded in paraffin. Sections (4 μm) were stained with hematoxylin and eosin (H&E) or Periodic acid-Schiff (PAS) for histological analysis. Serial sections were used for immunohistochemical analysis. Immunostaining was performed on unstained paraffin sections. First, the sections were deparaffinized and rehydrolyzed using 100% Xylol followed by a dilution series with isopropanol (100%, 90%, 70%). Antigen retrieval was performed by cooking the slides in Tris-EDTA buffer for 20 min (10 mM Tris Base, 1 mM EDTA solution, 0.05% Tween 20, pH 9.0). Blocking was done in a 5% bovine serum albumin (BSA), 0.1% Triton X-100 PBS solution for 1 h at room temperature. Primary and secondary antibodies were incubated at room temperature for 1 h and 30 min, respectively. BrdU staining required an additional HCl (4 M) treatment for 20 min. Primary antibodies were anti-Nanog (1:50 dilution; Abcam, ab80892), anti-Cdx2 (1:100 dilution; Biogenex, CDX2-88), anti-Klf4 (1:100 dilution; Santa Cruz, sc-20691), anti-β-catenin (1:100 dilution; BD Transduction Laboratories, 610154), and anti-BrdU (1:100 dilution; Developmental Studies Hybridoma Bank, G3G4). Secondary antibodies were Alexa Fluor 488 or Alexa Fluor 568 from Invitrogen (1:400 dilution). Slides were mounted with Vectashield Mounting Medium with Dapi (Vector H-1200) and analyzed by fluorescence microscopy.

BrdU labeling

BrdU (Sigma B5002) was injected intraperitoneally at a concentration of 30 mg/kg of body weight. Mice were sacrificed 2, 4, and 48 h after injection, and BrdU incorporation was detected by immunohistochemistry. Quantification of BrdU-positive cells was done using ImageJ.

Cell proliferation analysis

NIH 3T3 fibroblasts were cultured on a 12-well dish in a rich medium containing 10% BSA. 3×10^4 cells were infected with retroviral vectors expressing mouse Nanog cDNA or empty control vector. Cells were counted by hand on days 0, 2, 4, and 7.

Epithelial cell preparation

The intestine and colon were isolated from induced and uninduced tet-Nanog mice. The organs were washed with PBS and incised along their length. Samples were then incubated with PBS/EDTA (5 mM) at 4 °C for 30 min, followed by vigorous shaking and centrifugation at 500 rpm for 5 min. Pellets were resuspended in 0.25% trypsin/EDTA supplemented with 0.8 μg/μl DNase and incubated at 37 °C for 30 min. After digestion, samples were shaken and centrifuged at 1400 rpm for 10 min. Pellets were resuspended in DMEM Low Glucose medium and filtered twice through a 100-μm cell strainer and then twice through a 70-μm cell strainer. Single cells were obtained and used for follow-up experiments.

Chromatin immunoprecipitation (ChIP)

ChIP was performed as previously described (Marson et al., 2008) with some modifications. Intestinal and colonic epithelial cells were cross-linked with 1% formaldehyde for 10 min at room temperature, and chromatin was digested with micrococcal nuclease followed by 10 × 30-s pulses of sonication using Biorupter (Diagenode). Chromatin fragments, mainly mono- to trinucleosome in size, were immunoprecipitated with the antibodies against Nanog (A300-397A, Bethyl Laboratories) or normal rabbit IgG. The precipitated DNA was analyzed by using real-time PCR. For each experiment, the percentage of input was determined and normalized to the value obtained at two negative control regions within the intergenic spacer (IGS) of ribosomal DNA. All primers are listed in Table S1.

Quantitative real-time PCR

Reverse transcription was performed using the MMLV reverse transcriptase (USB) and Oligo-dT15 priming at 42 °C for 1 h followed by 60 °C heat inactivation for 10 min. A cDNA concentration equivalent to 50 ng of total RNA was used for the real-time polymerase chain reaction (PCR). Real-time PCR was performed with 2× Power SYBR Green PCR mix (ABI) and 0.375 μM of each primer in a total volume of 20 μl using the ABI 7300 cycler. Calculations were done using the ΔΔCt

method with two housekeeping genes as internal controls. The primers used are listed in Table S1.

Microarray analysis

RNA samples for the microarrays were prepared using QIAGEN RNeasy columns with on-column DNA digestion. 300 ng of total RNA per sample was used as input into a linear amplification protocol (Ambion), which involved synthesis of T7-linked double-stranded cDNA and 12 h of in vitro transcription incorporating biotin-labeled nucleotides. Purified and labeled cRNA was hybridized for 18 h onto MouseRef-8 v2 expression BeadChips (Illumina) following the manufacturer's instructions. After washing as recommended, the chips were stained with streptavidin-Cy3 (GE Healthcare) and scanned using the iScan reader (Illumina) and accompanying software. Samples were exclusively hybridized as biological replicates. The bead intensities were mapped to gene information using BeadStudio 3.2 (Illumina). Background correction was performed using the Affymetrix Robust Multi-array Analysis (RMA) background correction model (Irizarry et al., 2003). Variance stabilization was performed using the log2 scaling, and gene expression normalization was calculated with the method implemented in the lumi package of R-Bioconductor. Data post-processing and graphics was performed with in-house developed functions in Matlab. Hierarchical clustering of genes and samples was performed with one minus correlation metric and the unweighted average distance (UPGMA) (also known as group average) linkage method.

Flow cytometry

Cells then were stained with purified anti-mouse CD326 (Clone G8.8, eBioscience) and APC-conjugated donkey anti-rat secondary antibody (Jackson ImmunoResearch) and analyzed on a FACSAria cell sorter (BD Biosciences). Highly CD326-positive cells were isolated by fluorescence-activated cell sorting (FACS) using a 100-μm nozzle. Data analysis was done using FlowJo software (Tree Star).

Results

Generation of Nanog-inducible transgenic mice

Murine ES cells derived from mice of OG2 background were used to engineer Nanog-inducible ES cells. These ES cells carry an Oct4-GFP reporter construct, whose expression corresponds to that of the endogenous Oct4 and which is a valid reprogramming marker according to our previous studies (Boiani et al., 2002; Do and Schöler, 2004; Kim et al., 2008, 2009). A modified tetracycline-inducible system, first described by Anastassiadis et al. (2002) was used to drive inducible expression of the Nanog transgene (Fig. 1A) upon the addition of doxycycline and dexamethasone (Fig. S1 available online). A clonally derived Nanog-inducible ES cell line showed strong and rapid induction of the Nanog transgene after addition of dexamethasone and doxycycline (Fig. 1B). Using quantitative real-time PCR, full expression of the Nanog transgene was detected 3.5 h after induction. According to previous publications, induced tet-Nanog ES cells can be grown indefinitely in the absence of LIF (Chambers et al., 2003; Mitsui et al., 2003). The Oct4-GFP transgene, an indicator of pluripotency, remained highly active, and cells obtained a normal ES cell morphology when seeded back on a layer of irradiated mouse embryonic fibroblasts without LIF supplementation (Fig. 1C). This result indicated that the Nanog transgene was biologically functional. Transgenic mice were produced from this ES cell line by diploid morula aggregation and subsequent mating. Following intraperitoneal injection of doxycycline and dexamethasone, strong transgene induction was detected in nearly all major organs (Figs. 1D and E). The low induction level in the brain may be due to the difficulty of the ligands in passing through the blood–brain barrier, as previously observed in other tet-inducible mouse models (Hochedlinger et al., 2005; Anastassiadis et al., 2010). Interestingly, after induction with doxycycline and dexamethasone, Nanog expression levels in most organs exceeded those of wild-type ES cells (Fig. S1B).

Nanog expression leads to hyperplasia in the intestinal and colonic epithelium

To force Nanog expression, 3- to 6-week-old mice were injected intraperitoneally with doxycycline and dexamethasone every other day. Depending on the age, mice reacted well to treatment for up to 6 weeks, after which they became morbid and died. An initial screen of old mice treated for 6 weeks revealed that morphological changes were restricted to the intestinal tract. As shown in Fig. 2A, these mice showed significant extensions of the villi in the small intestine and outgrowths of the mucosa in the colon. These protrusions were examined pathologically and diagnosed as hyperplasia of the intestinal epithelium. Control mice carrying the irtTA did not show phenotypic changes of the intestinal tract after prolonged injection with doxycycline and dexamethasone. To further study the onset of the phenotype, 3-week-old mice were used for follow-up experiments. If Nanog interfered with the development of the gut epithelium, the young mice were expected to show a stronger or an earlier onset of the phenotype. As the young mice died within 3 weeks of treatment, the timeframe of the experiment was shortened to 2.5 weeks. Through quantification of villus length, we identified that the elongation of the villi was most significant in the duodenum and jejunum (Fig. 2B). After 7 days of Nanog induction, the villi had extended by almost 100% in the duodenum and jejunum, with no significant change in villus length in the ileum. This phenotypic effect became more prominent until day 9, after which time there was no significant change in villus length. Interestingly, the phenotype was reversible following termination of Nanog induction. Three weeks after Nanog withdrawal, the length of the villi was significantly reduced, approaching baseline levels of control mice. This shows that the observed extension was dependent upon continuous Nanog expression. The colon also showed signs of hyperplasia 9 days after induction (Fig. 2C). In the cecum, small outgrowths from the epithelial layer had started to form, consistent with the outgrowths we observed in the older mice that had been treated for 6 weeks. In comparison, the mucosa of the uninduced cecum was much

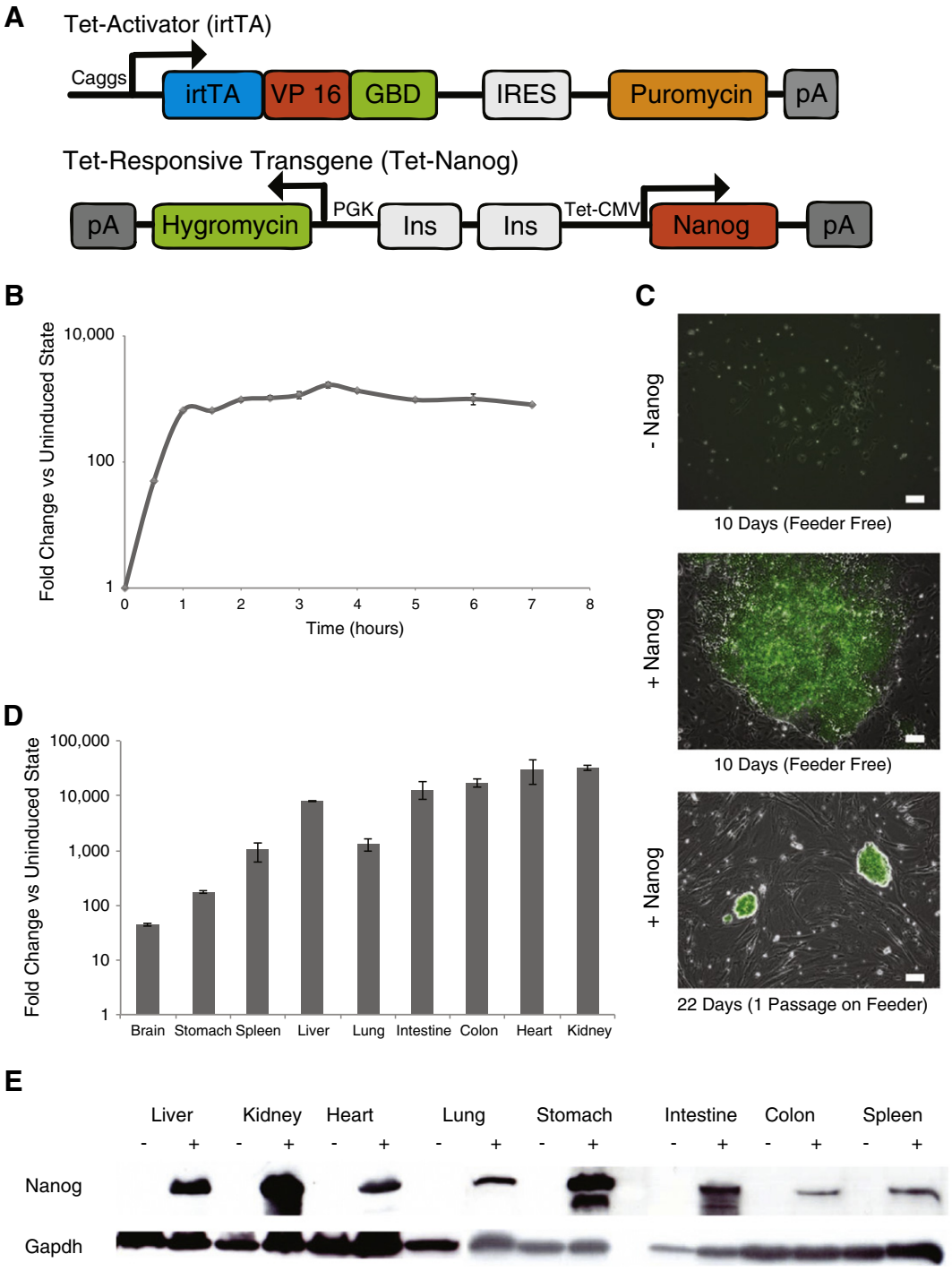

Figure 1 Characterization of Nanog-inducible mouse embryonic stem cells and mice. (A) Schematic overview of the transgenes used to produce the Nanog-inducible ES cells and mice. Both transgenes were randomly integrated into OG-2ES cells. An improved codon-optimized tetracycline transactivator fused to the glucocorticoid receptor ligand-binding domain was used. The Nanog transgene is under the control of a tetracycline-responsive CMV minimal promoter protected by two chicken beta globin insulators. The arrowheads mark the transcriptional start sites. irtTA, improved reverse tetracycline transactivator; VP16, viral protein 16; GBD, mutated glucocorticoid receptor ligand-binding domain; IRES, internal ribosomal entry site; pA, polyadenylation signal; Ins, chicken beta globin insulators. (B) Kinetics of Nanog transgene response to doxycycline and dexamethasone induction in ES cells. Nanog RNA levels were measured using quantitative real-time PCR, with levels normalized to those obtained using uninduced tet-Nanog ES cells. (C) Cultivation of tet-Nanog ES cells in the absence of LIF with and without the induction of Nanog transgene. GFP signal is representative of the endogenous Oct4 levels. (D) RNA levels of the Nanog transgene in different organs of tet-Nanog mice after intraperitoneal injection of dexamethasone and doxycycline. Levels in induced organs are normalized to those of in uninduced organs. (E) Western blot analysis of tet-Nanog mouse after Nanog transgene induction. + and − represent the induced state and the uninduced state, respectively. The bars in panels B and D reflect normalization errors. The scale bars in panel C are 100 μm.

smoother and looked more structured. PAS staining also revealed an underrepresentation of goblet cells within these outgrowths; however, this did not affect the total amount of goblet cells in the small intestine and colon (Fig. S3B). In the colon, the typical smooth colonic epithelium had become more ridged and had begun growing further into the lumen. As in the cecum, PAS staining of the colon showed a reduction in the amount of goblet cells within these outgrowths (Fig. 2C).

Increased proliferation rates in the crypt compartment causes hyperplasia in Nanog-induced mice

Several studies have shown that Nanog has an accelerating effect on the cell cycle, so we performed a proliferation assay on NIH 3T3 cells infected with Nanog to validate this (Zhang et al., 2005, 2009; Camp et al., 2009). Our results are consistent with previously published data, showing an enhanced rate of proliferation of NIH 3T3 cells infected with Nanog (Fig. 3A) (Zhang et al., 2005). Next, a BrdU staining of the small intestine and colon was performed to test the effect of Nanog on proliferation in vivo. An initial screen was performed on mice induced for 9 days with a 4-h BrdU pulse. Although the staining signal appeared stronger in Nanog-induced mice, no change in the location of the proliferating cells was revealed. All BrdU-positive cells were located in the crypt compartment (Fig. 3B). To further investigate the behavior of the proliferating cells, a time course of BrdU incorporation was performed. Mice were induced with Nanog for 7 days and then injected with BrdU. At different time points after the injection, BrdU incorporation was analyzed. Two hours after BrdU injection, stronger staining was observed within the crypt compartment of the Nanog-induced mice compared with the uninduced mice (Fig. 3C). Quantification revealed an 85% increase in BrdU-positive cells per crypt compared with control mice (Fig. 3C). This showed that ectopic Nanog expression influences the proliferation of naturally proliferating cells in the crypt compartment. To determine whether this corresponds to a faster repopulation of the villi in Nanog-induced mice, we examined BrdU incorporation at 48 h. In Nanog-induced mice, BrdU-stained cells had migrated to the top of the villus, while in control mice, the BrdU-stained cells had migrated only midway up the villi (Fig. 3D). Taken together, these results show that an increased proliferation of the crypt compartment correlates with an increased repopulation of the villi, suggesting that increased proliferation is a key component of the observed hyperplasia in Nanog-induced mice.

Ectopic Nanog expression leads to differential expression of genes in intestine and colon

To gain further insight into these changes on a molecular level, a global gene expression analysis was performed. Tissue samples exhibited heterogeneity, as observed by principal component analysis, with repeats of the small intestine in particular not clustering as well as the ones from the colon (Fig. 4E). Thus, it is possible that only changes in widely expressed genes could be picked up in our experiments. The scatter plot showed that Nanog expression led to 416 differentially expressed genes in the small intestine (Fig. 4C) and 408 in the colon (Fig. 4D). Some commonly up- and downregulated genes in both organs were identified, among them the key intestinal regulators Cdx2 and Klf4 (Figs. 4A–D). Both of these genes have been described to be tumor suppressors and are involved in the control of differentiation and growth of the intestinal epithelium (Garrett-Sinha et al., 1996; Shields et al., 1996; Beck et al., 1999; Katz et al., 2002; Bonhomme et al., 2003; McConnell et al., 2007; Gao et al., 2009). As a result, both Cdx2 and Klf4 are very interesting candidates for further investigations. To address the issue of heterogeneity in the whole tissue samples, an additional microarray on presorted intestinal and colonic epithelial cells was performed. As expected, the dendrogram of the sorted repeats showed a much higher degree of homogeneity compared with the whole tissue sample (Fig. S4A). However, as no additional candidate genes were found, the focus was on Cdx2 and Klf4 (Figs. S4B–D).

Nanog crosstalks with Cdx2 and Klf4 in the intestinal tract of mice

We evaluated Cdx2 repression with a Nanog overexpression time course, quantified by real-time PCR. Downregulation of Cdx2 in the small intestine and colon was observed throughout the entire 3-week time course (Figs. 5A and C). After 2–3 weeks of treatment, expression of Cdx2 was reduced to about 20% of its original level in the small intestine and down to 1% in the colon. In response to Nanog induction, downregulation of Klf4 expression followed the same trend, but was not as strong (Fig. S2). To determine whether the observed Cdx2 downregulation is a direct effect of Nanog expression, an expression profile was performed for the 12 h following Nanog induction. Cdx2 expression negatively correlated with Nanog expression (Figs. 5B and D), as both the small intestine and the colon showed a strong downregulation of Cdx2 within the first 6 h of Nanog expression (Figs. 5B and D). This effect was stronger in the colon, correlating with the findings of the microarray analysis and the 3-week real-time PCR time course (Figs. 4B, 5A, and C). Within the first 6 h of Nanog induction, a rapid and immediate downregulation in Klf4 expression was also observed. The degree of repression was similar in both the small intestine and colon (Figs. S3B and D). Next, double immunostaining was performed for Cdx2 and Nanog on treated versus untreated samples. The negative expression of Cdx2 in the epithelium of the small intestine was found to correlate with the strong Nanog expression throughout the entire villus (Fig. 5E). A strong reduction in Cdx2 protein was also found in the colon (Fig. 5E). However, as Nanog expression was not as uniform as in the small intestine, some cells remained positive for Cdx2. Repression of Cdx2 correlated with Nanog expression, as only cells that stained highly positive for Nanog were negative for Cdx2 (Fig. 5E). This further confirmed the strong dependence of Cdx2 expression levels on the presence of Nanog.

Nanog occupies Cdx2 and Klf4 regulatory elements in intestine and colon

To clarify whether the observed downregulation of Cdx2 and Klf4 in response to Nanog induction is a direct or an indirect effect, chromatin immunoprecipitation (ChIP) of Nanog was performed on primary intestinal and colonic epithelial cells.

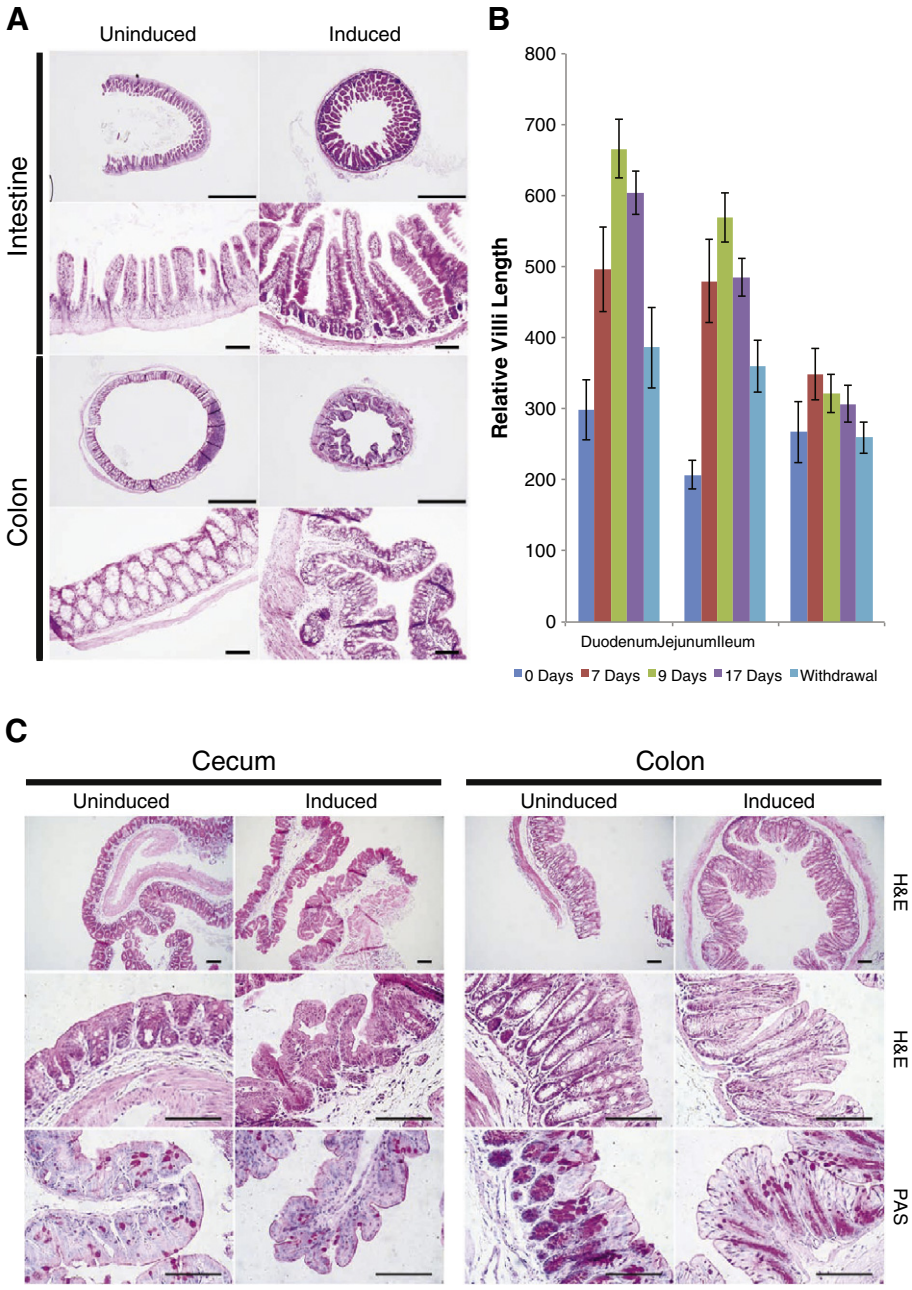

Figure 2 Histological analysis of hyperplasia in Nanog-induced mice. (A) H&E staining of the small intestine and colon after 6 weeks of Nanog induction. Hyperplasia is observed in the epithelium of the small intestine and colon, manifesting as an extension of the villi in the small intestine and villi-like outgrowths of the colonic epithelium into the lumen of the colon. (B) The length of the villi of the small intestine was measured and quantified in 3-week-old mice after an indicated time of Nanog induction. After 7 days of induction, Nanog was withdrawn and the cells were allowed to recover for 3 weeks without Nanog induction. The duodenum, jejunum, and ileum were analyzed separately. Villus length was scored from the end of the crypts to the end of the villi. (C) H&E and PAS staining of the cecum and colon after 9 days of Nanog induction in 3-week-old mice. Signs of outgrowths from the epithelial layer are present in the cecum and the colon. For quantification, the duodenum makes up the first 10% after the stomach, the jejunum the next 30%, and the ileum the remaining 60% to the cecum. Length of the villi was quantified on H&E-stained sections from the top of each villus until the beginning of the crypt using ImageJ. The error bars in panel B represent the standard deviation from the mean. The average numbers of counted villi in panel B are as follows: duodenum n = 18; jejunum n = 46; and ileum n = 104. The scale bars in panel A are 1000 μm for the lower magnification and 200 μm for the higher magnification. In panel C, the scale bars are 100 μm.

A previous transgenic study identified an enhancer located 8.5-kb upstream of the transcriptional start site that directs the expression of Cdx2 in intestinal cells (Benahmed et al., 2008). Interestingly, Nanog binds to the promoter (Region C) and upstream enhancer (Region A) of Cdx2 in both the small intestine and colon (Figs. 6B and D). Strong binding of Nanog

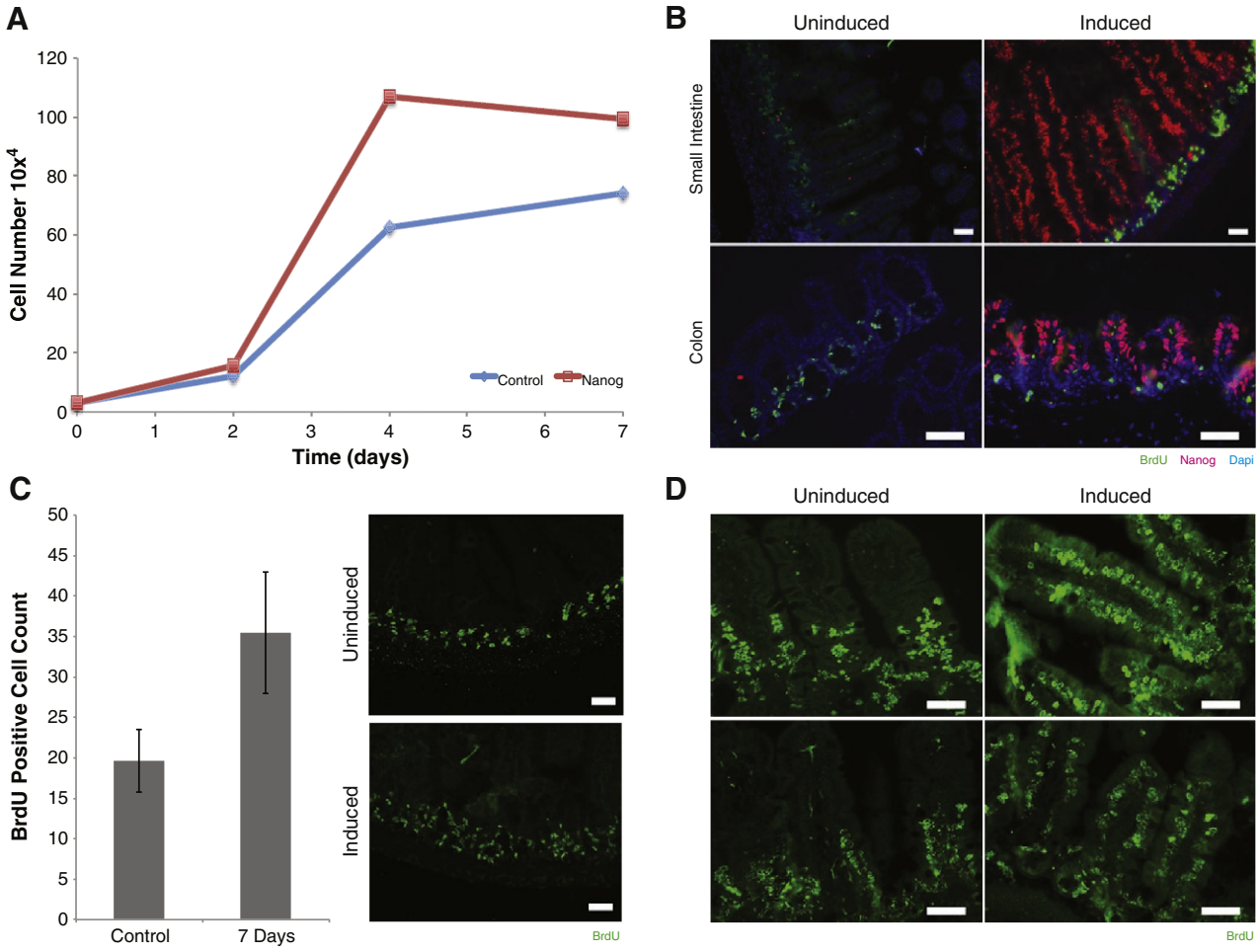

Figure 3 Effects of Nanog expression on proliferation in vitro and in vivo. (A) Proliferation curve of Nanog-expressing NIH 3T3 cells, compared with wild-type NIH 3T3 cells. (B) BrdU immunostaining of the small intestine and colon after a 4-h BrdU pulse. tet-Nanog mice induced for 9 days were compared with uninduced mice. (C) Analysis of BrdU incorporation after a 2-h BrdU pulse 7 days after of Nanog induction. The left panel shows a quantification of the BrdU-positive cell per crypt of each villus (control, n = 647; Nanog induced, n = 1028). The right-hand panel shows a representative image of BrdU staining in the intestine after a 2-h pulse. (D) Images show immunostaining of a 48-h BrdU pulse. The left-hand side shows uninduced control images; the right-hand side shows images of mice induced with Nanog for 7 days. The scale bars in panels B, C, and D are 50 μm.

was also observed downstream of Cdx2 (Region G), corresponding to a potential enhancer region identified in mouse (Watts et al., 2011) and human (Watts et al., 2011) The first intron (Regions D and E), which is occupied by Nanog in ES cells (Chen et al., 2008), also showed significant binding in both the small intestine and colon, suggesting that a common regulatory mechanism is active in these cells (Chen et al., 2009). Nanog also binds to the promoter region (Regions B and C) and upstream conserved region (Region A) of Klf4 in both the small intestine and colon (Figs. 7B and D). In contrast, the promoter region of β-catenin, which is highly expressed but not affected by Nanog induction, showed no enrichment, confirming the specific binding of Nanog to Cdx2 and Klf4 (Figs. 6C, E, 7C, and E).

Nanog does not effect the Wnt pathway in intestinal epithelium

The Wnt pathway plays an important role in the development of a normal and functional intestinal epithelium. Strong Wnt activation is often observed in intestinal tumors and has been reported to mediate for the phenotype observed after Oct4 induction (Hochedlinger et al., 2005). However, our microarray analysis did not reveal a strong upregulation of Wnt downstream target genes, such as CyclinD1 and c-Myc. As an active Wnt pathway can be identified by the nuclear localization of β-catenin, we then performed double immunostaining for Nanog and β-catenin. As shown in Fig. 5F, Nanog did not cause translocation of β-catenin into the nucleus of epithelial cells in the colon and small intestine. This finding demonstrates that Nanog does not affect the activity of the Wnt pathway, excluding a contribution of Wnt to the observed phenotype.

Discussion

We have generated and characterized a Nanog-inducible mouse with high Nanog expression levels in most major organs. Contrary to what we expected, prolonged Nanog

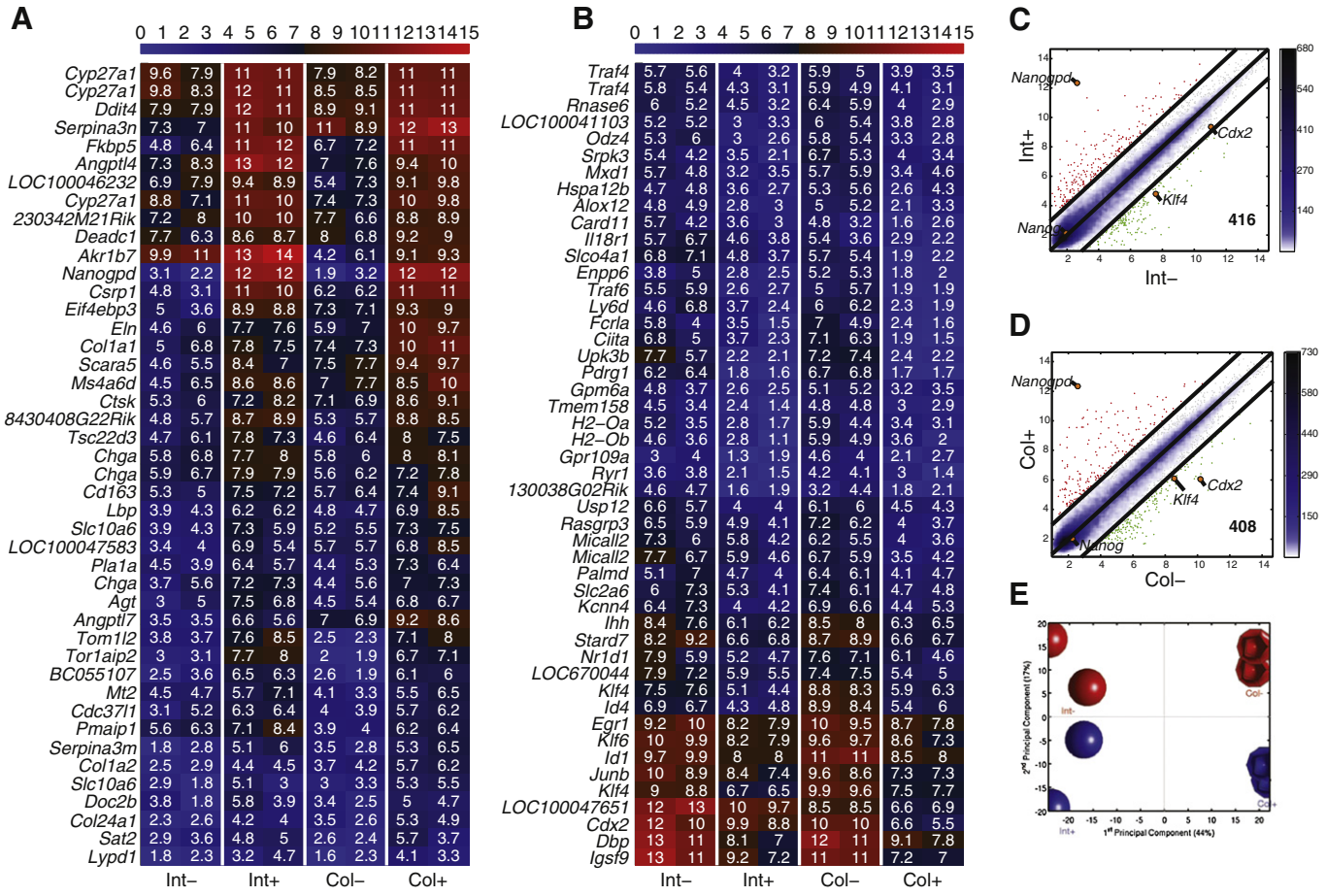

Figure 4 Global gene expression comparison for small intestine and colon after Nanog induction. (A) Heatmap of upregulated genes common to both the small intestine and colon after Nanog induction. Int−, uninduced small intestine; Int+, induced small intestine; Col−, uninduced colon; Col+, induced colon. (B) Heatmap of downregulated genes common to both the small intestine and colon after Nanog induction. Int−, uninduced small intestine; Int+, induced small intestine; Col−, uninduced colon; Col+, induced colon. (C) Pairwise scatter plot of uninduced vs Nanog-induced small intestine. Int−, uninduced small intestine; Int+, induced small intestine. The Nanogpd probe corresponds to the tet-Nanog transgenes, and the Nanog probe to the endogenous Nanog gene. (D) Pairwise scatter plot of uninduced vs Nanog-induced colon. Col−, uninduced colon; Col+, induced colon. The Nanogpd probe corresponds to the tet-Nanog transgenes, and the Nanog probe to the endogenous Nanog gene. (E) Principal component analysis of microarray data. The 1st principal component (PC1) captures 44% of the gene expression variability and the 2nd principal component (PC2) captures 17% of the variability. Panels A through D represent gene expression levels in a $\log_2$ scale.

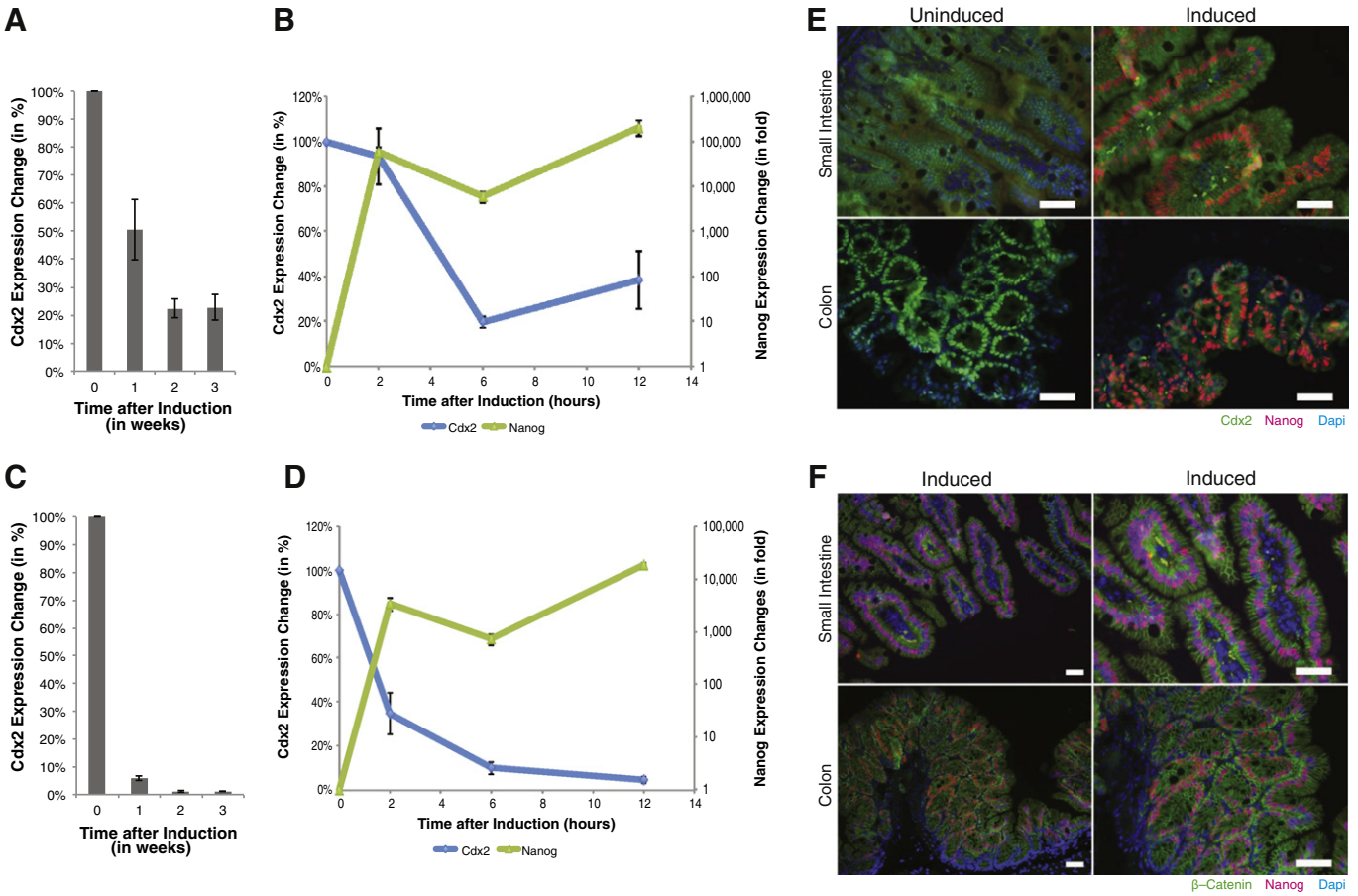

Figure 5 Effect of ectopic Nanog expression on Cdx2 and β-catenin. (A) Quantitative real-time PCR analysis of Cdx2 levels in the small intestine in a 3-week time course of Nanog overexpression. (B) Immediate effects of Nanog expression on Cdx2 expression levels in the small intestine, quantified via real-time PCR analysis. (C) Quantitative real-time PCR analysis of Cdx2 levels in the colon in a 3-week time course of Nanog overexpression. (D) Immediate effects of Nanog expression on Cdx2 expression levels in the colon, quantified via real-time PCR analysis. (E) Immunostaining for Cdx2 after 9 days of Nanog overexpression in the small intestine and colon. (F) Immunostaining for β-catenin after 9 days of Nanog overexpression in the small intestine and colon. The bars in panels A through D represent the normalization error. The scale bars in panels E and F are 50 μm.

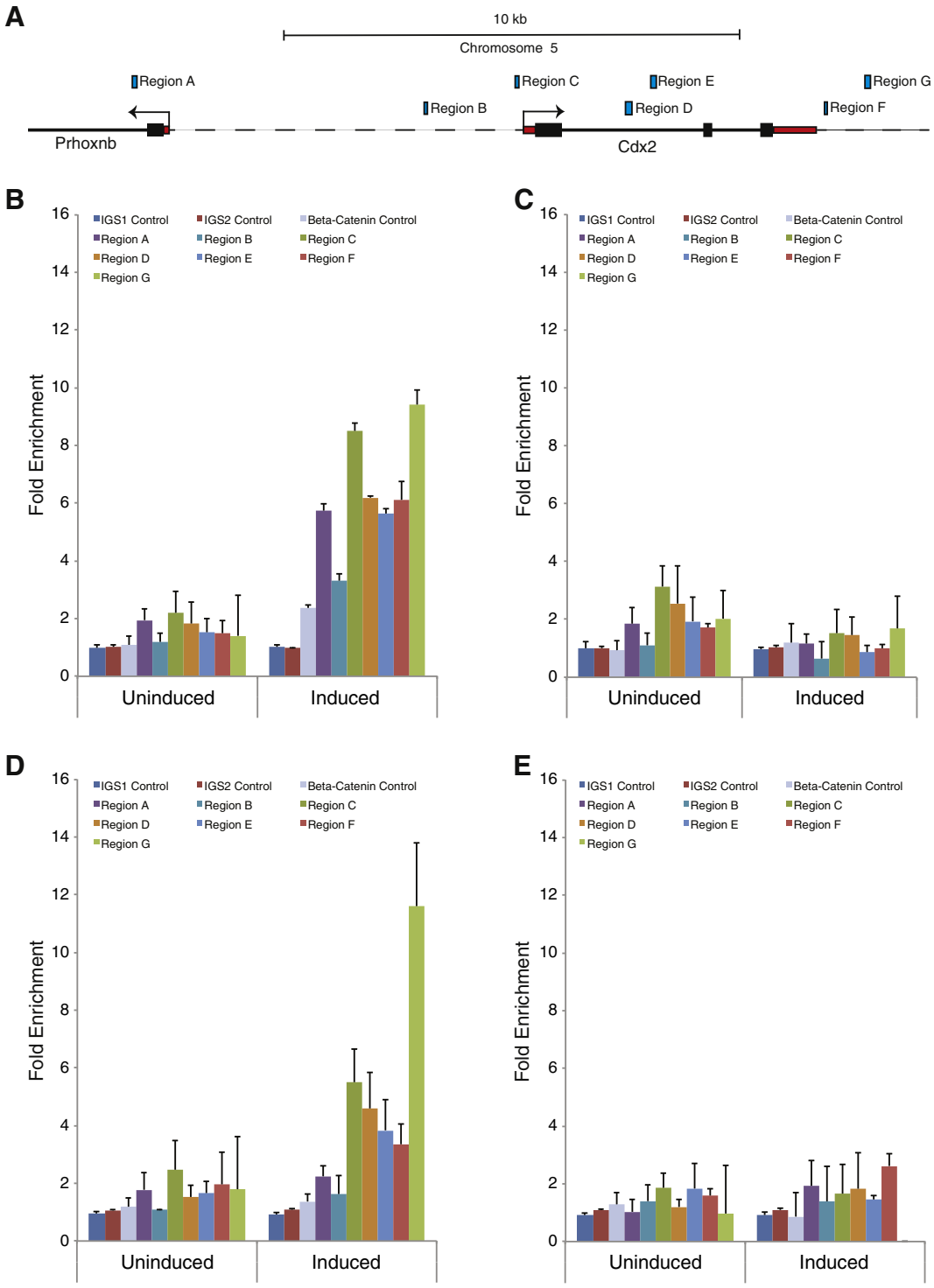

Figure 6 ChIP analysis of Nanog on Cdx2 regulatory elements. (A) Schematic overview of the murine Cdx2 locus. The red fields indicate the 3′ and 5′ untranslated regions, large black field are exons, small black lines are introns, and dotted lines represent intergenic regions. The blue fields show the PCR-amplified regions for the ChIP analysis. Candidate regions were picked within the Cdx2 regulatory regions based on previous publications and on well-conserved regions up- and downstream of the transcriptional start sites. (B) ChIP-PCR data for the small intestine using a Nanog antibody. Fold enrichment over negative control regions (IGS1 and IGS2) is shown. (C) Control ChIP-PCR data for the small intestine using control IgG. (D) ChIP-PCR data for the colon using a Nanog antibody. (E) Control ChIP-PCR data for the colon using control IgG.

expression led to phenotypic changes that were restricted to the small intestine and colon, leaving other major organs unaffected. Although Nanog does not play a role in the formation of the gastrointestinal tract during embryonic development, its overexpression during adulthood leads to hyperplasia of the epithelium and abnormal morphology of

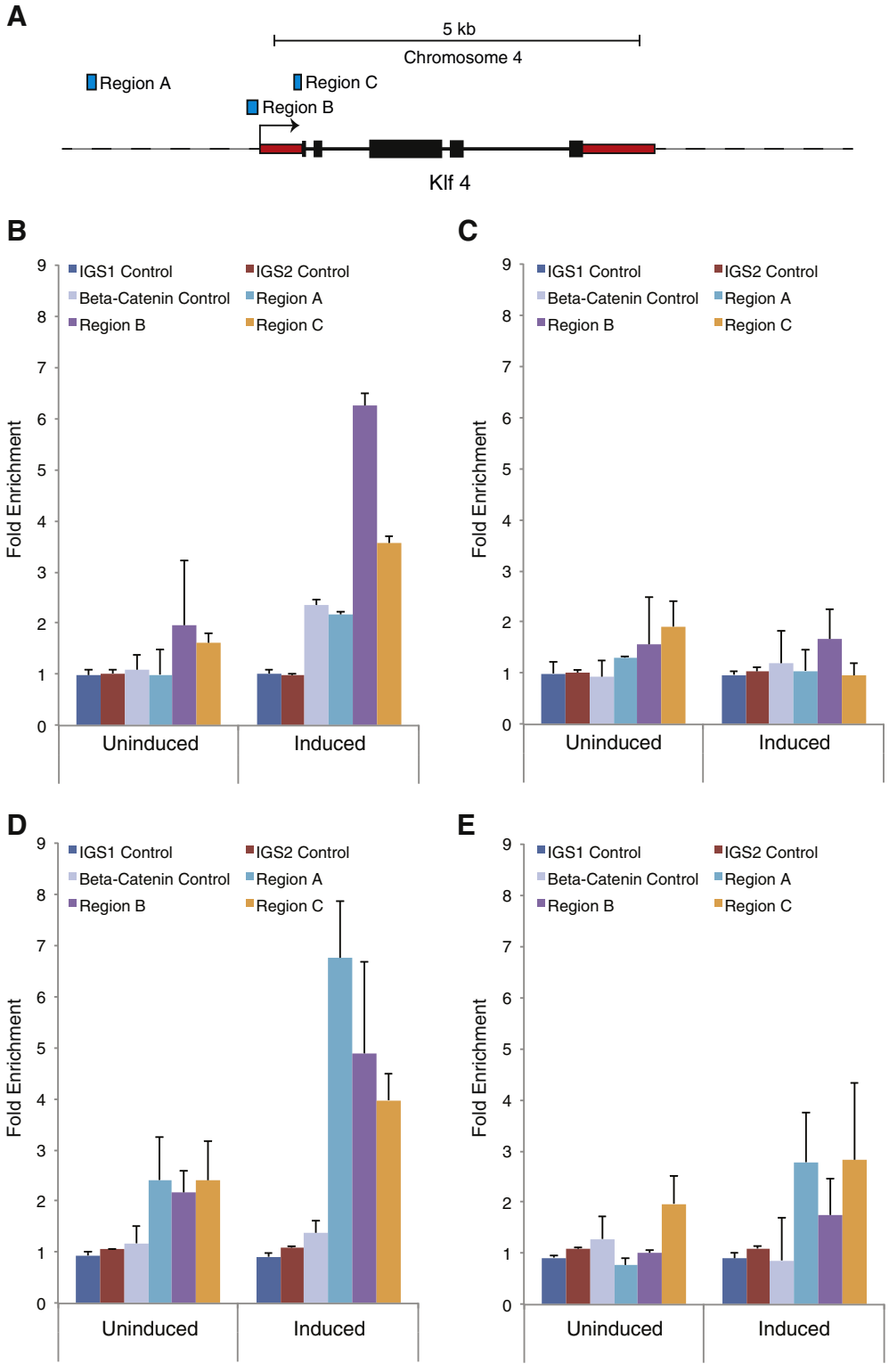

Figure 7 ChIP analysis of Nanog on Klf4 regulatory elements. (A) Schematic overview of the murine Klf4 locus. The red fields indicate the 3′ and 5′ untranslated regions, large black field are exons, and small black lines are introns. The blue fields show the PCR-amplified regions for the ChIP analysis. Candidate regions within the Klf4 regulatory regions were based on well-conserved regions upstream of the transcriptional start sites. (B) ChIP-PCR data for the small intestine using a Nanog antibody. (C) Control ChIP-PCR data for the small intestine using control IgG. (D) ChIP-PCR data for the colon using a Nanog antibody. (E) Control ChIP-PCR data for the colon using control IgG.

the mucosal architecture (Fig. 2A). Hyperplastic outgrowths were always observed but they never led to the formation of adenomas or carcinomas. To gauge whether mice that had not reached adulthood would show a stronger response to Nanog expression, newly weaned 3-week-old mice were analyzed. Though these mice were not able to withstand the treatment for longer than 2–3 weeks, they showed signs of hyperplasia after only 7 days. The villi of the small intestine doubled in length on day 7 and continued to grow until day 9, after which time the extension leveled off. Three weeks after withdrawal of dexamethasone and doxycycline, downregulation of Nanog expression and reduced villus length were once again observed, showing that the hyperplasia is dependent upon continuous Nanog expression (Fig. 2B). The colon also showed signs of hyperplasia after 9 days of Nanog induction. As shown in Fig. 2C, the colonic mucosa, which has a typical flat morphology, developed outgrowths that were pathologically identified as hyperplasia of the colonic epithelium. Moreover, a reduction in the number of goblet cells within these outgrowths was observed by PAS staining. Forced expression of Nanog in NIH 3T3 cells and human ES cells has been shown to promote entry into the S-phase of the cell cycle, enhancing the rate of proliferation (Zhang et al., 2005, 2009). To determine whether Nanog influences the proliferation of the intestinal tract, a time course of BrdU incorporation was performed after 7 days of Nanog overexpression. Indeed, 2 h after BrdU administration, an additional 85% of cells in the crypts showed proliferation in response to Nanog treatment (Fig. 3C). This is an interesting finding, as the intestinal stem cells residing in the crypts are responsible for the repopulation of the villi with differentiated cells. The next time point, 48 h post–BrdU administration, further showed that cells labeled with BrdU migrated faster up the crypt compartment in the Nanog-induced mice. The possibility that the observed signal was due to dormant epithelial cells that had initiated proliferation was excluded, as the BrdU-labeled cells were not scattered around the villi but were all in line with the natural migration pathway from the crypt up the villi. Furthermore, no proliferation of the typically dormant cells was observed between 2 and 48 h (see representative example in Fig. 3B). These results clearly demonstrated that altered proliferation within the crypt compartment plays a dominant role in the development of the observed hyperplasia. The morbidity and deaths of 6-week-old mice upon Nanog induction might be caused by a combination of doxycycline/dexamethasone/ethanol treatment and malabsorption related to the intestinal phenotype.

By microarray analysis and subsequent immunostaining, significant downregulation of both Cdx2 and Klf4 was observed in the small intestine and colon. Both genes play an important role in the development and maintenance of a functional intestinal epithelium. The finding that other organs did not exhibit phenotypic changes upon Nanog overexpression suggested that Cdx2 and Klf4 might be key factors in the development of the described phenotype.

Using quantitative real-time PCR, a strong reduction of Cdx2 and Klf4 expression levels was found within the first 6 h of Nanog induction, demonstrating that Nanog is a direct repressor of these two genes (Figs. 5A–D and S2). ChIP further revealed binding of Nanog to the regulatory elements of Cdx2 and Klf4 in primary cells isolated from the small intestine and colon (Figs. 6 and 7). These results, together with the expression data, clearly demonstrate that Nanog binds to Cdx2 and Klf4 and represses their transcription.

Cdx2 is a transcription factor that regulates numerous intestine-specific genes and mediates many cellular processes, such as cell differentiation, proliferation, adhesion, migration, and tumorigenesis (Ee et al., 1995; Chawengsaksophak et al., 1997; Beck et al., 1999, 2003; Aoki et al., 2003; Bonhomme et al., 2003; Gao et al., 2009). During early embryonic development, Cdx2 expression is repressed by Nanog and restricted to the extraembryonic lineage (Chen et al., 2009). The downregulation of Cdx2 in the Nanog-expressing intestinal epithelium clearly demonstrates that Nanog suppression of Cdx2 is conserved from embryonic development to adulthood. A Cdx2 homozygous knockout phenotype is lethal, whereas heterozygous mice spontaneously form adenomatous polyps, particularly in the proximal colon, correlating with the appearance of the epithelial outgrowths we identified after Nanog induction (Chawengsaksophak et al., 1997). The adenomas in the heterozygous knockout mice were shown to be negative for Cdx2, and mouse chimeric models and conditional Cdx2 knockout models have further strengthened the validity of these findings (Beck et al., 2003; Gao et al., 2009).

The downregulation of Klf4 is another interesting effect of Nanog overexpression. Klf4 has also been shown to act as a tumor suppressor and its absence to lead to induction of hyperplasia in the gastric epithelium (Katz et al., 2005). Nanog binding to the Klf4 promoter was demonstrated by ChIP analysis, revealing that Nanog itself exerts a repressive action upon Klf4. Furthermore, Cdx2 has been shown to be an activator of Klf4 (Mahatan et al., 1999; Dang et al., 2001), suggesting that Nanog likely affects Klf4 expression directly by binding to the Klf4 promoter and indirectly by suppressing Cdx2 expression.

Our in vivo study of Nanog overexpression identified the transcription factor to be an inducer of hyperplasia and a repressor of both Cdx2 and Klf4 expression in the adult intestinal epithelium. Although Cdx2 and Klf4 expression has been previously associated with hyperplasia and adenoma formation, we could not find evidence that it leads to tumor formation in our mice. As mice heterozygous for Cdx2 form adenomatous polyps at 3 months of age (Chawengsaksophak et al., 1997), it is possible that the timeframe of our experiments was too short to observe initiation of tumor growth. However, unlike Oct4, Nanog does not affect the Wnt pathway (Hochedlinger et al., 2005), further reducing the possibility that Nanog exhibits oncogenic properties and induces intestinal and/or colonic tumor formation. In line with our findings a recent study of a NanogP8 homolog transgenic mouse model demonstrated absence of spontaneous tumor formation and actual inhibition of tumor development in a two-stage chemical carcinogenesis model (Badeaux et al., 2013).

Taken together, the findings of this study suggest that Nanog has an influence on the intestinal and colonic architecture but does not have a functional role in tumor initiation. However, due to the increased proliferation of intestinal cells and the repressive effect on both Cdx2 and Klf4, Nanog may further enhance growth of established intestinal tumors. The fact that, despite being widely expressed by the inducible tet-system, phenotypic alterations were only observed in the intestine and colon, argues

against Nanog's functional involvement in initiation of tumor formation in many different tissues. We therefore conclude that Nanog cannot be classified as an oncogene and that positive detection of Nanog expression in tumor samples may be due to secondary events.

Supplementary data to this article can be found online at http://dx.doi.org/10.1016/j.scr.2014.08.001.

Acknowledgments

We are very grateful and would like to thank Ingrid Gelker for cell culture, Bärbel Schäfer for histology, Gabriele Verberk, Martina Sinn, and Boris Burr for PCR analysis, and Areti Malapetsas for editing the manuscript. Furthermore, we thank the whole staff of the animal facility, particularly Ludger Recker, Christin Schmitz, and Alexandra Buehler. The work presented here was funded by the Max Planck Society and the Federal Ministry of Education and Research (BMBF grant 01GN0811).

Database linking

The data discussed in this publication have been deposited in NCBI's Gene Expression Omnibus and are accessible through GEO Series accession number GSE GSE31413.

(http://www.ncbi.nlm.nih.gov/geo/query/acc.cgi?token=rfopdesiwmqiepk&acc=GSE31413)

References

Al-Hajj, M., Wicha, M.S., Benito-Hernandez, A., Morrison, S.J., Clarke, M.F., 2003. Prospective identification of tumorigenic breast cancer cells. Proc. Natl. Acad. Sci. U. S. A. 100, 3983–3988.

Alldridge, L., Metodieva, G., Greenwood, C., Al-Janabi, K., Thwaites, L., Sauven, P., Metodiev, M., 2008. Proteome profiling of breast tumors by gel electrophoresis and nanoscale electrospray ionization mass spectrometry. J. Proteome Res. 7, 1458–1469.

Anastassiadis, K., Kim, J., Daigle, N., Sprengel, R., Schöler, H.R., Stewart, A.F., 2002. A predictable ligand regulated expression strategy for stably integrated transgenes in mammalian cells in culture. Gene 298, 159–172.

Anastassiadis, K., Rostovskaya, M., Lubitz, S., Weidlich, S., Stewart, A.F., 2010. Precise conditional immortalization of mouse cells using tetracycline-regulated SV40 large T-antigen. Genesis 48, 220–232.

Aoki, K., Tamai, Y., Horiike, S., Oshima, M., Taketo, M.M., 2003. Colonic polyposis caused by mTOR-mediated chromosomal instability in Apc+/Delta716 Cdx2+/− compound mutant mice. Nat. Genet. 35, 323–330.

Atlasi, Y., Mowla, S.J., Ziaee, S.A.M., Bahrami, A.-R., 2007. OCT-4, an embryonic stem cell marker, is highly expressed in bladder cancer. Int. J. Cancer 120, 1598–1602.

Badeaux, M.A., Jeter, C.R., Gong, S., Liu, B., Suraneni, M.V., Rundhaug, J., Fischer, S.M., Yang, T., Kusewitt, D., Tang, D.G., 2013. In vivo functional studies of tumor-specific retrogene NanogP8 in transgenic animals. Cell Cycle 12, 2395–2408.

Beachy, P.A., Karhadkar, S.S., Berman, D.M., 2004. Tissue repair and stem cell renewal in carcinogenesis. Nature 432, 324–331.

Beck, F., Chawengsaksophak, K., Luckett, J., Giblett, S., Tucci, J., Brown, J., Poulsom, R., Jeffery, R., Wright, N.A., 2003. A study of regional gut endoderm potency by analysis of Cdx2 null mutant chimaeric mice. Dev. Biol. 255, 399–406.

Beck, F., Chawengsaksophak, K., Waring, P., Playford, R.J., Furness, J.B., 1999. Reprogramming of intestinal differentiation and intercalary regeneration in Cdx2 mutant mice. Proc. Natl. Acad. Sci. U. S. A. 96, 7318–7323.

Ben-Porath, I., Thomson, M.W., Carey, V.J., Ge, R., Bell, G.W., Regev, A., Weinberg, R.A., 2008. An embryonic stem cell-like gene expression signature in poorly differentiated aggressive human tumors. Nat. Genet. 40, 499–507.

Benahmed, F., Gross, I., Gaunt, S.J., Beck, F., Jehan, F., Domon Dell, C., Martin, E., Kedinger, M., Freund, J.N., Duluc, I., 2008. Multiple regulatory regions control the complex expression pattern of the mouse Cdx2 homeobox gene. Gastroenterology 135, 1238–1247 (e3).

Boiani, M., Eckardt, S., Schöler, H.R., McLaughlin, K.J., 2002. Oct4 distribution and level in mouse clones: consequences for pluripotency. Genes Dev. 16, 1209–1219.

Bonhomme, C., Duluc, I., Martin, E., Chawengsaksophak, K., Chenard, M.-P., Kedinger, M., Beck, F., Freund, J.-N., Domon-Dell, C., 2003. The Cdx2 homeobox gene has a tumour suppressor function in the distal colon in addition to a homeotic role during gut development. Gut 52, 1465–1471.

Boyer, L.A., Lee, T.I., Cole, M.F., Johnstone, S.E., Levine, S.S., Zucker, J.P., Guenther, M.G., Kumar, R.M., Murray, H.L., Jenner, R.G., et al., 2005. Core transcriptional regulatory circuitry in human embryonic stem cells. Cell 122, 947–956.

Bussolati, B., Bruno, S., Grange, C., Ferrando, U., Camussi, G., 2008. Identification of a tumor-initiating stem cell population in human renal carcinomas. FASEB J. 22, 3696–3705.

Camp, E., S nchez-S nchez, A.V., Garc a-Espa a, A., DeSalle, R., Odqvist, L., Enrique O'Connor, J., Mullor, J.L., 2009. Nanog regulates proliferation during early fish development. Stem Cells 27, 2081–2091.

Cantz, T., Key, G., Bleidissel, M., Gentile, L., Han, D.W., Brenne, A., Schöler, H.R., 2008. Absence of OCT4 expression in somatic tumor cell lines. Stem Cells 26, 692–697.

Chambers, I., Colby, D., Robertson, M., Nichols, J., Lee, S., Tweedie, S., Smith, A., 2003. Functional expression cloning of Nanog, a pluripotency sustaining factor in embryonic stem cells. Cell 113, 643–655.

Chawengsaksophak, K., James, R., Hammond, V.E., Köntgen, F., Beck, F., 1997. Homeosis and intestinal tumours in Cdx2 mutant mice. Nature 386, 84–87.

Chen, L., Yabuuchi, A., Eminli, S., Takeuchi, A., Lu, C.-W., Hochedlinger, K., Daley, G.Q., 2009. Cross-regulation of the Nanog and Cdx2 promoters. Nat. Publ. Group 19, 1052–1061.

Chen, X., Xu, H., Yuan, P., Fang, F., Huss, M., Vega, V.B., Wong, E., Orlov, Y.L., Zhang, W., Jiang, J., et al., 2008. Integration of external signaling pathways with the core transcriptional network in embryonic stem cells. Cell 133, 1106–1117.

Chiou, S.-H., Wang, M.-L., Chou, Y.-T., Chen, C.-J., Hong, C.-F., Hsieh, W.-J., Chang, H.-T., Chen, Y.-S., Lin, T.-W., Hsu, H.-S., et al., 2010. Coexpression of Oct4 and Nanog enhances malignancy in lung adenocarcinoma by inducing cancer stem cell-like properties and epithelial–mesenchymal transdifferentiation. Cancer Res. 70, 10433–10444.

Chiou, S.-H., Yu, C.-C., Huang, C.-Y., Lin, S.-C., Liu, C.-J., Tsai, T.-H., Chou, S.-H., Chien, C.-S., Ku, H.-H., Lo, J.-F., 2008. Positive correlations of Oct-4 and Nanog in oral cancer stem-like cells and high-grade oral squamous cell carcinoma. Clin. Cancer Res. 14, 4085–4095.

Dang, D.T., Mahatan, C.S., Dang, L.H., Agboola, I.A., Yang, V.W., 2001. Expression of the gut-enriched Krüppel-like factor (Krüppel-like factor 4) gene in the human colon cancer cell line RKO is dependent on CDX2. Oncogene 20, 4884–4890.

Do, J.T., Schöler, H.R., 2004. Nuclei of embryonic stem cells reprogram somatic cells. Stem Cells 22, 941–949.

Ee, H.C., Erler, T., Bhathal, P.S., Young, G.P., James, R.J., 1995. Cdx-2 homeodomain protein expression in human and rat

colorectal adenoma and carcinoma. Am. J. Pathol. 147, 586–592.

Ezeh, U.I., Turek, P.J., Reijo, R.A., Clark, A.T., 2005. Human embryonic stem cell genes OCT4, NANOG, STELLAR, and GDF3 are expressed in both seminoma and breast carcinoma. Cancer 104, 2255–2265.

Gao, N., White, P., Kaestner, K.H., 2009. Establishment of intestinal identity and epithelial–mesenchymal signaling by Cdx2. Dev. Cell 16, 588–599.

Garrett-Sinha, L.A., Eberspaecher, H., Seldin, M.F., de Crombrugghe, B., 1996. A gene for a novel zinc-finger protein expressed in differentiated epithelial cells and transiently in certain mesenchymal cells. J. Biol. Chem. 271, 31384–31390.

Gillis, A.J., Stoop, H., Biermann, K., van Gurp, R.J., Swartzman, E., Cribbes, S., Ferlinz, A., Shannon, M., Oosterhuis, J.W., Looijenga, L.H., 2011. Expression and interdependencies of pluripotency factors LIN28, OCT3/4, NANOG and SOX2 in human testicular germ cells and tumours of the testis. Int. J. Androl. 34 (4 Pt 2), e160–e174.

Hochedlinger, K., Yamada, Y., Beard, C., Jaenisch, R., 2005. Ectopic expression of Oct-4 blocks progenitor-cell differentiation and causes dysplasia in epithelial tissues. Cell 121, 465–477.

Hubbard, S.A., Gargett, C.E., 2010. A cancer stem cell origin for human endometrial carcinoma? Reproduction 140, 23–32.

Irizarry, R.A., Bolstad, B.M., Collin, F., Cope, L.M., Hobbs, B., Speed, T.P., 2003. Summaries of Affymetrix GeneChip probe level data. Nucleic Acids Res. 31, e15.

Jeter, C.R., Badeaux, M., Choy, G., Chandra, D., Patrawala, L., Liu, C., Calhoun-Davis, T., Zaehres, H., Daley, G.Q., Tang, D.G., 2009. Functional evidence that the self-renewal gene NANOG regulates human tumor development. Stem Cells 27, 993–1005.

Katz, J.P., Perreault, N., Goldstein, B.G., Actman, L., McNally, S.R., Silberg, D.G., Furth, E.E., Kaestner, K.H., 2005. Loss of Klf4 in mice causes altered proliferation and differentiation and precancerous changes in the adult stomach. Gastroenterology 128, 935–945.

Katz, J.P., Perreault, N., Goldstein, B.G., Lee, C.S., Labosky, P.A., Yang, V.W., Kaestner, K.H., 2002. The zinc-finger transcription factor Klf4 is required for terminal differentiation of goblet cells in the colon. Development 129, 2619–2628.

Kim, J.B., Sebastiano, V., Wu, G., Araúzo-Bravo, M.J., Sasse, P., Gentile, L., Ko, K., Ruau, D., Ehrich, M., van den Boom, D., et al., 2009. Oct4-induced pluripotency in adult neural stem cells. Cell 136, 411–419.

Kim, J.B., Zaehres, H., Wu, G., Gentile, L., Ko, K., Sebastiano, V., Araúzo-Bravo, M.J., Ruau, D., Han, D.W., Zenke, M., et al., 2008. Pluripotent stem cells induced from adult neural stem cells by reprogramming with two factors. Nature 454, 646–650.

Lin, T., Ding, Y.-Q., Li, J.-M., 2012. Overexpression of Nanog protein is associated with poor prognosis in gastric adenocarcinoma. Med. Oncol. 29, 878–885.

Lobo, N.A., Shimono, Y., Qian, D., Clarke, M.F., 2007. The biology of cancer stem cells. Annu. Rev. Cell Dev. Biol. 23, 675–699.

Mahatan, C.S., Kaestner, K.H., Geiman, D.E., Yang, V.W., 1999. Characterization of the structure and regulation of the murine gene encoding gut-enriched Krüppel-like factor (Krüppel-like factor 4). Nucleic Acids Res. 27, 4562–4569.

Marson, A., Levine, S.S., Cole, M.F., Frampton, G.M., Brambrink, T., Johnstone, S., Guenther, M.G., Johnston, W.K., Wernig, M., Newman, J., et al., 2008. Connecting microRNA genes to the core transcriptional regulatory circuitry of embryonic stem cells. Cell 134, 521–533.

Masui, S., Nakatake, Y., Toyooka, Y., Shimosato, D., Yagi, R., Takahashi, K., Okochi, H., Okuda, A., Matoba, R., Sharov, A.A., et al., 2007. Pluripotency governed by Sox2 via regulation of Oct3/4 expression in mouse embryonic stem cells. Nat. Cell Biol. 9, 625–635.

McConnell, B.B., Ghaleb, A.M., Nandan, M.O., Yang, V.W., 2007. The diverse functions of Krüppel-like factors 4 and 5 in epithelial biology and pathobiology. Bioessays 29, 549–557.

Meng, H.-M., Zheng, P., Wang, X.-Y., Liu, C., Sui, H.-M., Wu, S.-J., Zhou, J., Ding, Y.-Q., Li, J.-M., 2010. Overexpression of nanog predicts tumor progression and poor prognosis in colorectal cancer. Cancer Biol. Ther. 9.

Mitsui, K., Tokuzawa, Y., Itoh, H., Segawa, K., Murakami, M., Takahashi, K., Maruyama, M., Maeda, M., Yamanaka, S., 2003. The homeoprotein Nanog is required for maintenance of pluripotency in mouse epiblast and ES cells. Cell 113, 631–642.

Nagy, A., Gertsenstein, M., Vintersten, K., Behringer, R., 2002. Manipulating the Mouse Embryo: A Laboratory Manual, Third ed. Cold Spring Harbor Laboratory Press.

O'Brien, C.A., Pollett, A., Gallinger, S., Dick, J.E., 2007. A human colon cancer cell capable of initiating tumour growth in immunodeficient mice. Nature 445, 106–110.

Reya, T., Morrison, S.J., Clarke, M.F., Weissman, I.L., 2001. Stem cells, cancer, and cancer stem cells. Nature 414, 105–111.

Saiki, Y., Ishimaru, S., Mimori, K., Takatsuno, Y., Nagahara, M., Ishii, H., Yamada, K., Mori, M., 2009. Comprehensive analysis of the clinical significance of inducing pluripotent stemness-related gene expression in colorectal cancer cells. Ann. Surg. Oncol. 16, 2638–2644.

Shields, J.M., Christy, R.J., Yang, V.W., 1996. Identification and characterization of a gene encoding a gut-enriched Krüppel-like factor expressed during growth arrest. J. Biol. Chem. 271, 20009–20017.

Stingl, J., Caldas, C., 2007. Molecular heterogeneity of breast carcinomas and the cancer stem cell hypothesis. Nat. Rev. Cancer 7, 791–799.

Summers, M.C., McGinnis, L.K., Lawitts, J.A., Raffin, M., Biggers, J.D., 2000. IVF of mouse ova in a simplex optimized medium supplemented with amino acids. Hum. Reprod. 15, 1791–1801.

Szabó, P.E., Hübner, K., Schöler, H., Mann, J.R., 2002. Allele-specific expression of imprinted genes in mouse migratory primordial germ cells. Mech. Dev. 115, 157–160.

Tai, M.-H., Chang, C.-C., Kiupel, M., Webster, J.D., Olson, L.K., Trosko, J.E., 2005. Oct4 expression in adult human stem cells: evidence in support of the stem cell theory of carcinogenesis. Carcinogenesis 26, 495–502.

Wang, J., Rao, S., Chu, J., Shen, X., Levasseur, D.N., Theunissen, T.W., Orkin, S.H., 2006. A protein interaction network for pluripotency of embryonic stem cells. Nature 444, 364–368.

Watts, J.A., Zhang, C., Klein-Szanto, A.J., Kormish, J.D., Fu, J., Zhang, M.Q., Zaret, K.S., 2011. Study of FoxA pioneer factor at silent genes reveals Rfx-repressed enhancer at Cdx2 and a potential indicator of esophageal adenocarcinoma development. PLoS Genet. 7, e1002277.

Wen, J., Park, J.Y., Park, K.H., Chung, H.W., Bang, S., Park, S.W., Song, S.Y., 2010. Oct4 and Nanog expression is associated with early stages of pancreatic carcinogenesis. Pancreas 39, 622–626.

Wong, D.J., Liu, H., Ridky, T.W., Cassarino, D., Segal, E., Chang, H.Y., 2008. Module map of stem cell genes guides creation of epithelial cancer stem cells. Cell Stem Cell 2, 333–344.

Ye, F., Zhou, C., Cheng, Q., Shen, J., Chen, H., 2008. Stem-cell-abundant proteins Nanog, Nucleostemin and Musashi1 are highly expressed in malignant cervical epithelial cells. BMC Cancer 8, 108.

Yoshimizu, T., Sugiyama, N., De Felice, M., Yeom, Y.I., Ohbo, K., Masuko, K., Obinata, M., Abe, K., Schöler, H.R., Matsui, Y., 1999. Germline-specific expression of the Oct-4/green fluorescent protein (GFP) transgene in mice. Dev. Growth Differ. 41, 675–684.

Zhang, J., Wang, X., Chen, B., Suo, G., Zhao, Y., Duan, Z., Dai, J., 2005. Expression of Nanog gene promotes NIH3T3 cell proliferation. Biochem. Biophys. Res. Commun. 338, 1098–1102.

Zhang, S., Balch, C., Chan, M.W., Lai, H.-C., Matei, D., Schilder, J.M., Yan, P.S., Huang, T.H.-M., Nephew, K.P., 2008. Identification and characterization of ovarian cancer-initiating cells from primary human tumors. Cancer Res. 68, 4311–4320.

Zhang, X., Neganova, I., Przyborski, S., Yang, C., Cooke, M., Atkinson, S.P., Anyfantis, G., Fenyk, S., Keith, W.N., Hoare, S.F., et al., 2009. A role for NANOG in G1 to S transition in human embryonic stem cells through direct binding of CDK6 and CDC25A. J. Cell Biol. 184, 67–82.

Zhang, Y., Buchholz, F., Muyrers, J.P., Stewart, A.F., 1998. A new logic for DNA engineering using recombination in *Escherichia coli*. Nat. Genet. 20, 123–128.

Zhang, Y., Muyrers, J.P., Testa, G., Stewart, A.F., 2000. DNA cloning by homologous recombination in *Escherichia coli*. Nat. Biotechnol. 18, 1314–1317.